

# Flutter of a Soft Plate in Channel Flow (Fundamental Study on Palatal Flutter)

by

Takashi YUMINO\*<sup>1</sup>, Tsuneo SAITO\*<sup>2</sup>, Keiichi SASAKI\*<sup>3</sup>  
and Yoshimichi TANIDA\*<sup>4</sup>

(received on Mar. 28,2002 & accepted on July 10,2002)

## Abstract

Regarding the palatal flutter in snoring, experimental and theoretical studies are carried out for the flutter of a soft plate placed in a channel flow. The results show that (1)flutter occurs with an oscillation of travelling-wave mode beyond a critical flow velocity, (2)the channel walls act to promote flutter, whereas the hard plate attached in front of the soft plate acts to suppress flutter, although both of those effects are rather slight, and (3)flutter could be predicted theoretically by taking account of the mechanical damping of the plate. It is noted in the experiment that, once flutter occurs, the soft plate oscillates with large amplitude, and a hysteresis is observed, in which the flutter does not cease until the flow velocity is reduced to be much lower than the flutter velocity.

*Keywords: Flutter, Snoring, Soft plate, Palate, Channel flow*

## 1. Introduction

Recently, attention has been progressively paid on the mechanism of generation of snoring, which would be sometimes fatal<sup>(1)</sup>. The snoring is considered to be caused mainly by the self-excited oscillation of the soft palate in narrow airway. So, it would be important to study the palatal flutter from aerodynamic point of view, but only a few works have been done till now. Huang<sup>(2)</sup> first carried out experimental and theoretical studies on the snoring systematically to analyze the palatal flutter. He showed that flutter of the soft palate occurred in a travelling-wave mode of oscillation and could be predicted by the flutter analysis of an isolated aerofoil. His study, however, did not take account of the effects of the airway wall and the hard palate attached fore to the soft palate. Under impetus from Huang's work, one of the present authors presented a computational method for a soft plate oscillating in two-dimensional subsonic channel flows and showed that flutter could occur in travelling-wave oscillation mode<sup>(3)</sup>.

The purpose of the present paper is to elucidate the characteristics of the palatal flutter experimentally and theoretically, taking account of the effects of the airway wall and the hard palate. Experiments are carried out for soft plates of natural, urethane and  $\alpha$ -gel rubbers, which are set in vertical or horizontal channel. Theoretical approach is also performed for predicting the palatal

flutter.

## 2. Experiment

### 2.1 Experimental setup and procedures

Figure 1 shows the experimental setup used in the present study, which consists of a rectangular duct (50 mm wide, 40/60/80 mm high), a settling chamber and a blower. The duct is set either vertically or horizontally, in order to examine the gravity effect. A soft plate is allocated on the duct axis, being clamped to a hard plate which is 60-100 mm long, 10 mm thick, and fully spanned in the duct.

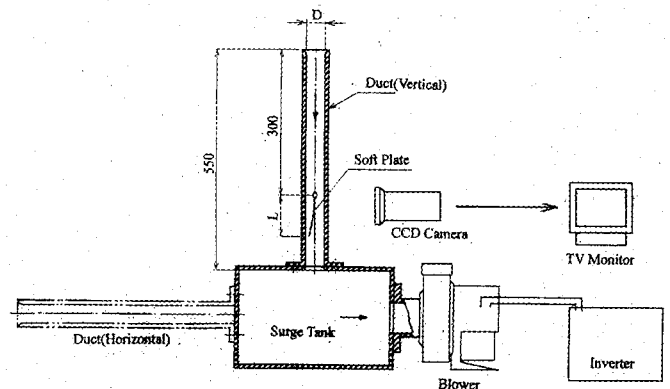


Fig. 1 Experimental setup

In the present study are used several kinds of soft plates of natural, urethane and  $\alpha$ -gel rubbers, which are 60-150 mm long, 16/32/48 mm wide and 1 mm or 2 mm ( $\alpha$ -gel) thick, as shown in Fig.2.

\* 1 Associate Professor, Department of Mechanical Engineering.  
\* 2 Yokohama Plant, Nissan Motor Co., LTD  
\* 3 Medical Information System Division, Hitachi Medical Corporation.  
\* 4 Former Professor, Department of Prime Mover Engineering.

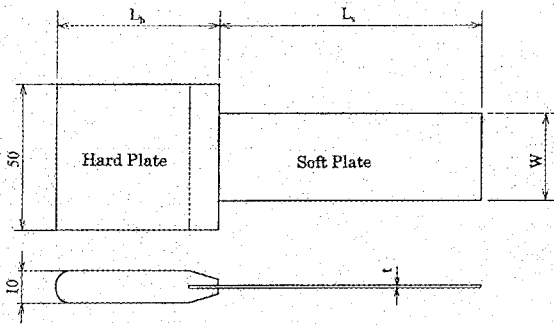


Fig. 2 Model Plate

A steady flow is generated in the duct by the blower. Increasing the flow velocity causes the soft plate to vibrate at flutter-on velocity  $U_f$  and then, decreasing the flow velocity leads it to stop again at flutter-off velocity  $U_s$ . Flow velocity in the duct is measured by a hot-wire anemometer, and oscillation mode of the soft plate is observed by high-speed video camera (Kodak Ektapro 1000).

2.2 Experimental results

2.2.1 Mode of oscillation The natural frequency can not be defined clearly in the oscillation of the soft plate. Then, when hanging and swinging the soft plate freely, its oscillating frequency

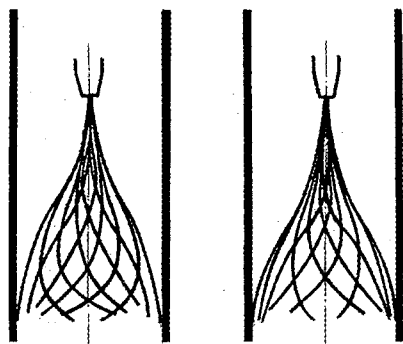
Table 1 Properties of Plates

$L_s=100\text{mm}, W=16/32/48\text{mm}$

Plate	Mass per Unit Area kg/m <sup>2</sup>	Nat. Freq. $F_n$ 1/s	Log. Decrement $\delta$
Natural Rubber*1	1.84	2.80	0.442
Urethane Rubber*1	1.44	5.00	0.450
$\alpha$ -gel Rubber*2	2.00	1.90	0.129

\*1 : Thickness=1mm  
\*2 : Thickness=2mm

will be called here as the natural frequency. The swinging mode is similar to the first cantilever mode, but it damps out abruptly. The properties of each rubber plate of  $L_s=100\text{mm}$  are given in Table 1<sup>(4)</sup>.



(a) Natural Rubber Plate (b)  $\alpha$ -gel Rubber Plate

Fig. 3 Oscillation in Flutter  
 $D=60\text{mm}, L_h=70\text{mm}, L_s=100\text{mm}$

When the soft plate is fluttering in flow, its oscillation mode is entirely different from the free oscillation mode, as shown in Fig.3, which illustrates the oscillation at every 30 degrees in one cycle, taken from the pictures of high-speed video camera. Once the plate embarks on flutter, it oscillates in large amplitude, eventually hitting the channel walls. It is noted that the oscillation mode has a travelling-wave form with a travelling velocity  $V$  less than the flow

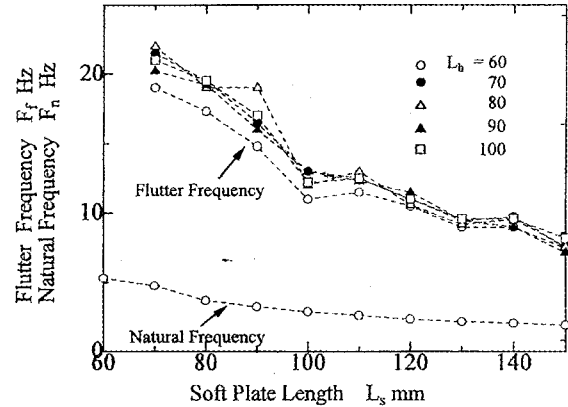


Fig. 4 Natural and Flutter Frequencies  
Vertical Duct Type, Natural Rubber  
 $D=60\text{mm}, W=32\text{mm}$

velocity  $U$ . It is likely that the trailing edge oscillates with phase lag  $\phi = \omega L_s/V = 2.0\text{rad}$  behind the fixed end, irrespective of the length of the soft plate. The oscillation mode mentioned above is similar to that obtained by Huang<sup>(2)</sup>. The flutter frequency  $F_f$  is nearly proportional to the natural frequency  $F_n$ , but it is several times as large as the latter, as shown in Fig.4. In the case of an elastic plate such as a metal one, the oscillation may occur with a frequency near around its natural frequency, but it is not the case for a soft plate.

2.2.2 Flutter velocity Figures 5 to 7 give typical results of the flutter velocity for the natural rubber plate, showing that longer plate falls into and recovers from flutter at lower flow velocities.

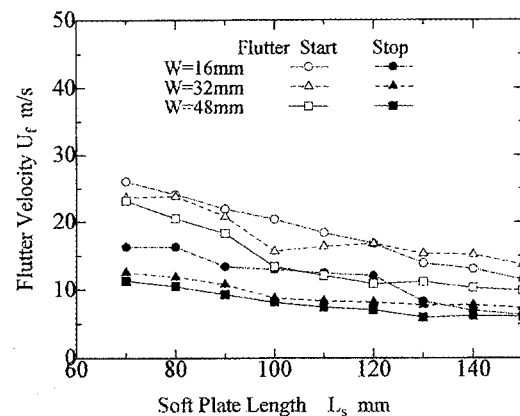


Fig. 5 Effect of Plate Geometry on Flutter  
Vertical Duct Type, Natural Rubber  
 $D=60\text{mm}, L_h=60\text{mm}$

It is striking that, once flutter occurs, it does not stop until the flow velocity is reduced much below the flutter velocity, such as  $U_s = 0.5 U_f$ . This hysteresis may be attributed to the non-linear aerodynamic characteristics of the soft plate oscillating with large amplitude. In the case of wide plates, such as  $W=48\text{mm}$ , slight drop of flow velocity is observed just after flutter occurs, that may be attributed to the blockage of flow due to large oscillation of the plate.

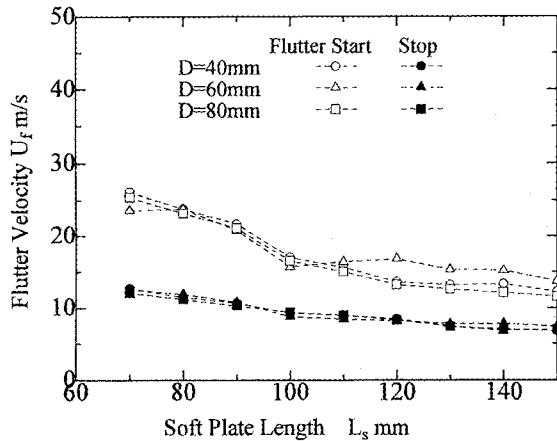


Fig.6 Effect of Channel Walls on Flutter  
Vertical Duct type, Natural Rubber  
 $W=32\text{mm}$ ,  $L_h=60\text{mm}$

Figure 5 shows that decrease of the plate width raises the flutter-on/-off velocity. It is considered that narrower plate width which makes larger gaps between the plate and duct side-walls brings about the divergence of flow and reduces the exciting flow

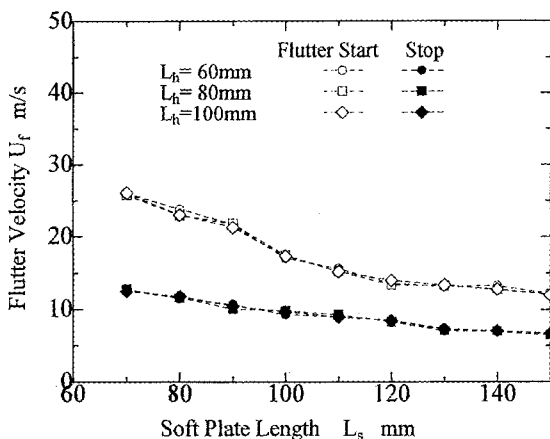


Fig.7 Effect of Hard Plate on Flutter  
Vertical Duct type, Natural Rubber  
 $W=40\text{mm}$ ,  $W=32\text{mm}$

force, as in the case of an aerofoil of finite span<sup>(5)</sup>. Figure 6 shows the effect of the channel height on the flutter velocity. For any plate length, the flutter velocity, both start and stop, are nearly independent of the channel height. For flutter start, that is presumably because the channel wall effect would be small for the

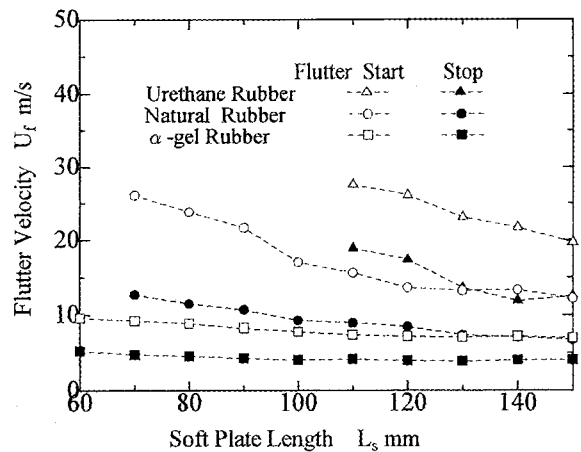


Fig.8 Effect of Plate Material on Flutter  
Vertical Duct type, Natural Rubber  
 $D=40\text{mm}$ ,  $W=32\text{mm}$ ,  $L_h=60\text{mm}$

oscillation of the soft plate with rather short wavelength comparable to the channel height, but no clear description could be made for flutter stop, when the violent oscillation bringing about the flow blockage would be closely related to the channel height.

Figure 7 shows the effect of the hard plate attached fore to the soft plate. The hard plate, too, does not give any significant effect on the flutter velocity, both start and stop. The hard plate is just similar as a spoiler, but it is far from the dominant part of the soft plate of large amplitude, so its effect would be rather small.

Figure 8 shows a comparison of the cases of the urethane and  $\alpha$ -gel rubbers with that of the natural rubber. Comparing with each other, the flutter velocity is nearly proportional to the natural frequency of plate, but the flutter characteristics are similar as a whole. The flutter velocity is not given for short urethane-rubber plates here, because the capacity of the blower is too small to increase the flow velocity to cause flutter of short urethane rubber plate.

No marked difference is observed between the vertical and horizontal cases, except for some of the  $\alpha$ -gel rubber plates. The thin  $\alpha$ -gel rubber plate is very flexible, so it bends down sluggishly on the lower duct wall in the horizontal case, that may lead to larger flow velocity for flutter.

Using the flutter velocity and frequency, the flutter reduced frequency  $(\omega L_s/U_f)$ , is obtained, as shown in Fig.9 for the natural-rubber plate. The flutter reduced frequency  $(\omega L_s/U_f)$  is around 0.5 in the cases of natural and urethane rubbers, and around 0.6 in the case of  $\alpha$ -gel rubber. Table 1 shows that all of the rubbers have nearly the same mass, but the logarithmic decrement of the  $\alpha$ -gel rubber is much small as compared with the others. Hence, for the  $\alpha$ -gel rubber, the low mechanical damping is considered to raise the flutter reduced frequency, as discussed later.

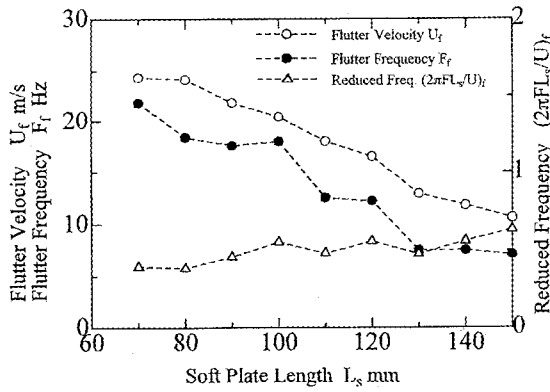


Fig.9 Flutter Reduced Frequency  
Vertical Duct type, Natural Rubber  
 $D=60\text{mm}$ ,  $W=48\text{mm}$ ,  $L_s=70\text{mm}$

Figure 9 shows that the flutter reduced frequency increases slightly as the plate length increases (or decreases), whereas Fig.6 shows no clear effect of the channel walls (or  $D/L_s$ ). It looks that these results of Fig.6 and Fig.9 conflict somewhat with each other, but Fig.9 is given for a constant plate width, so that longer plate may promote the three-dimensionality of flow, which reduces flutter velocity or increases flutter reduced frequency<sup>(5)</sup>. Hence, it could be said approximately that  $D/L_s$  and  $L_w/l_s$  have no significant effects on the occurrence of flutter, although they would be closely related to the noise generation in snoring.

### 3. Theoretical Approach

#### 3.1 Formulation

As mentioned above, the soft plate falls into flutter with large amplitude in travelling wave mode, which causes significant hysteresis between flutter-on and -off velocities. However, flutter starts with a oscillation of small amplitude, so the small perturbation analysis could be applied to estimate the flutter velocity. The details of the analysis used here are referred to Ref.3, but as for incompressible flow.

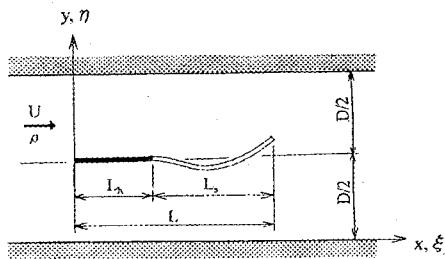


Fig.10 Model Plate

Figure 10 shows a fundamental model, in which a thin plate placed in two-dimensional channel oscillates with a frequency  $\omega$  in incompressible flow with small amplitude. Here,  $U$  is the flow velocity,  $\rho$  is the density of fluid,  $L$  is the total length of the plate ( $=L_1+L_2$ ),  $D$  is the channel height, and  $(x, y)$  and  $(\xi, \eta)$  are the

coordinates, in which  $(\xi, \eta)$  is related to the plate position (generally taken as  $0 \leq \eta \leq D$ ). Further,  $p$  is the pressure and  $t$  is the time.

Solving the linearized Euler equation of motion with the continuity equation, then the plate can be represented by a sheet of doublets of strength  $A(\xi)\exp(i\omega t)$ , with their axes perpendicular to the plate. The doublet strength is directly proportional to the pressure jump across the plate. That is,

$$A(\xi)\exp(i\omega t) = \frac{p_u - p_l}{\rho U^2} \quad (1)$$

where  $p_u$  and  $p_l$  denote the pressures on the upper and lower surfaces of the plate.

The upwash velocity on the plate  $(x, y)$  induced by the doublet  $(\xi, \eta)$  and its images is then given

$$v_a(x, \eta; \xi, \eta) = \frac{UA(\xi)}{d}\exp(i\omega t)\left[ (S_0 + S_1 + S_2) + \{1 + \text{sgn}(x - \xi)\}\exp\left\{-\frac{ik}{b}(x - \xi)\right\}S_3 \right] \quad (2)$$

Where

$$k = \frac{\omega b}{U}, \quad b = \frac{L}{2}, \quad q = \frac{\pi}{d}|x - \xi|, \quad p_\eta = \frac{\pi\eta}{d}$$

$$S_0 = \frac{1}{4}\text{sgn}(x - \xi)\sinh q \left( \frac{1}{\cosh q - 1} - \frac{1}{\cosh q - \cos 2p_\eta} \right)$$

$$S_1 = i \frac{dk}{4\pi b} \log \left( \frac{\cosh q - \cos 2p_\eta}{\cosh q - 1} \right)$$

$$S_2 = \sum_{v=1}^{\infty} \left[ \frac{v}{\text{sgn}(x - \xi)v - i \frac{dk}{\pi b}} - \left\{ \text{sgn}(x - \xi) + i \frac{dk}{\pi b v} \right\} \right] \times \exp(-vq) \sin^2 v p_\eta$$

$$S_3 = \pi a \left\{ \coth \pi a - \frac{\cosh a(\pi - 2p_\eta)}{\sinh \pi a} \right\}; \quad a = \frac{dk}{\pi b}$$

Here,  $S_0$  gives the quasi-steady component and  $S_3$  describes the contribution of the shed wake vortex conveyed downstream by the primary flow.

Integrating Eq.(2) over the plate gives the velocity induced on  $y = \eta$  by the whole doublets of the plate.

$$v(x, \eta) = \int_0^L v_d(x, \eta; \xi, \eta) d\xi, \quad x=0 \sim L \quad (3)$$

Assuming that the plate is oscillating with the displacement  $f(x) \exp(i\omega t)$ , the boundary condition is given as

$$v(x, \eta) = \left( \frac{\partial}{\partial t} + U \frac{\partial}{\partial x} \right) \{ f(x) \exp(i\omega t) \} \quad (4)$$

From Eqs.(2)~ (4) the doublet distribution  $A(\xi)$  can be obtained for a given mode of oscillation. In calculations, the doublet distribution function  $A(\xi)$  is expressed by the Glauert series, which satisfies the singularity at the leading edge and the Kutta condition at the trailing edge of the plate. Calculations are carried out for a finite number ( $N$ ) of control points, and the first  $N$  coefficients of the Glauert series are obtained.

For a given mode of oscillation, the instability is predicted from the energy input integrated over the plate,

$$E = \int_0^{2\pi/\omega} \int_0^L [A(\xi) \exp(i\omega t)]_R \left[ \frac{\partial}{\partial t} \{ f(\xi) \exp(i\omega t) \} \right]_R d\xi dt \quad (5)$$

where the suffix  $R$  denotes the real part of complex function.  $E$  is the aerodynamic work done to keep a given oscillation of the plate, so  $E > 0$  gives positive aerodynamic damping to suppress the oscillation and  $E < 0$  gives negative damping to cause flutter.

### 3.2 Numerical Results

As in the experiment, the plate is assumed to consist of two parts, fore hard one ( $L_h$ ) and aft soft one ( $L_s$ ), or,  $L = L_h + L_s$ , being allocated on channel axis ( $\eta = D/2$ ), as shown in Fig.10.

Here will be considered the case of a soft plate oscillating with the first cantilever mode but with a phase lag travelling downstream. Then,

$$\left. \begin{aligned} f(x) \exp(i\omega t) &= 0, & x &= 0 \sim L_h \\ f(x) \exp(i\omega t) &= C \left( \frac{\cosh \beta \tilde{x} - \cos \beta \tilde{x}}{\cosh \beta L_s + \cos \beta L_s} \right. \\ &\quad \left. - \frac{\sinh \beta \tilde{x} - \sin \beta \tilde{x}}{\sinh \beta L_s + \sin \beta L_s} \right) \exp \left\{ i\omega \left( t - \frac{\tilde{x}}{V} \right) \right\}, & x &= L_h \sim L \end{aligned} \right\} \quad (6)$$

where  $\tilde{x}$  is the distance from the fixed end of the soft plate,  $V$  the travelling-wave velocity, and  $\beta L_s = 0.60\pi$ , which satisfies  $\cos \beta L_s = -1/\cosh \beta L_s$ . The phase lag at the free end is given by  $\phi = \omega L_s/V$ . The local amplitude is normalized by the free-end amplitude. Figure 11 gives a travelling wave given by Eq.(6) for the phase lag  $\phi = 2.0$ , which agrees well with the real ones (Fig.3).

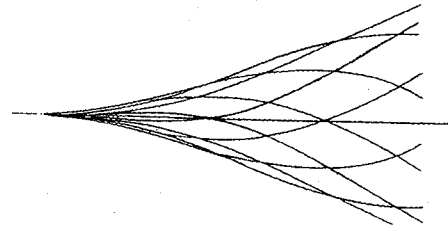


Fig.11 Travelling-Wave Oscillation of a soft plate

Calculations show that the standing-wave oscillation ( $\phi = 0$  or  $U/V = 0$ ) is always stable, but the travelling-wave oscillation becomes unstable by the negative energy input or negative damping below a critical reduced frequency, leading to the onset of flutter. In the following, the phase lag is taken as  $\phi = 2.0$  referring to the experimental results.

In the case with no mechanical damping, the flutter reduced frequency  $(\omega L_s/U)_f$  is given for  $E$  being zero. Figures 12 and 13 show the effects of the channel height  $D$  in the case with no hard plate ( $L_h = 0$ ) and the hard plate  $L_h$  in the case where the channel height is one-half of the soft plate length ( $D/L_s = 0.5$ ), respectively. It is seen that the channel walls act to raise the flutter reduced frequency, whereas the hard plate acts to reduce the flutter reduced frequency, although both of these effects are rather slight so as to be neglected. The plots in Fig.12 are the experimental results of the flutter reduced frequency obtained by Huang for a thin plastic sheet<sup>(2)</sup>.

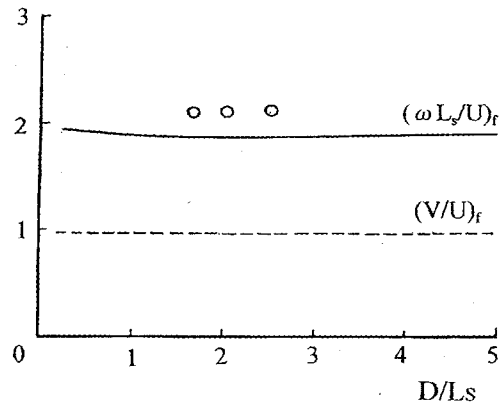


Fig.12 Effect of Channel Height  
 $L_h = 0.0$ ;  $\circ$ :Huang

He also estimated the travelling-wave velocity to be nearly equal to the flow velocity. His results agree well with those of the present calculation. This agreement would be attributed to the use of a thin plastic sheet by Huang, which may have small mechanical damping, as described below.

Comparing Figs.12 and 13 with Figs.6 and 7, the calculated results for the case of no mechanical damping agree with the

#### 4. Conclusion

Experimental and theoretical studies on flutter of a soft plate in channel flow are carried out, and the results obtained are summarized as follows.

Experimental results:

- (1) Beyond a critical flow velocity, flutter of a soft plate occurs in a traveling-wave oscillation mode with large amplitude so as to hit the channel walls.
- (2) Once flutter occurs, it does not stop until the flow velocity is reduced much below the flutter velocity, that is, there exists a remarkable hysteresis between flutter start and stop.
- (3) There are no significant effects of the channel walls and the hard plate attached fore to the soft plate on both flutter start and stop.

Calculated results:

- (4) As (3) in experiments, there are no significant effects of the channel wall and the hard plate, although the flutter reduced frequency slightly increases for smaller channel height and hard plate length.
- (5) The flutter reduced frequency obtained for the case of no mechanical damping is three to four times as much as the experimental one for rubber plate.

Concluding Remarks:

The present analysis treats the two-dimensional flow with small perturbations, so it would be well applied to the occurrence of flutter of a soft plate with no mechanical damping, as shown in Fig.12. For predicting the flutter velocity precisely, however, it would be indispensable to estimate the mechanical damping of the plate materials beforehand.

The results obtained shows that, for given conditions, the flutter reduced frequency is given rather definitely. So, in order to suppress flutter of soft plate or increase flutter velocity, it would be effective to increase the natural frequency of the soft plate or to stiffen the soft plate, that may easily applied to suppress the palatal flutter or snoring.

The hysteresis between flutter start and stop is also very interesting but remained to be elucidated. Besides, real hard and soft plates are thick and three-dimensional, so simulation model should be considered in both experiments and calculation.

#### References

- (1) Jannett, S., Snoring and its Treatment, British Medical J. 289(1984), p.335~336.
- (2) Huang, L., Acoustic Control for Men and Machineds, PhD Thesis, University of Cambridge (1992).
- (3) Tanida, Y., Stability of a Soft Plate in Channel Flow (Aerodynamic Aspects of Palatal Flutter), JSME Intl. J. (B) 44-1(2001), p.8~13.
- (4) Sasaki, K., Study on the Self-Excited Oscillation of Elastic Plates in Two-Dimensional Channel Flows, Master-Degree Thesis, Tokai Univ. (1999). (in Japanese)
- (5) Bisplinghoff, R.L., Ashley, H. and Halfman, R.L., Aeroelasticity, Addison Wesley Publ. Co. (1955).

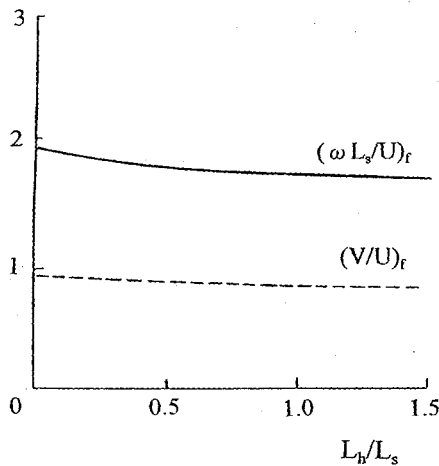


Fig.13 Effect of Hard Plate

$D/L_s=0.5$

experimental ones qualitatively. That is, both experimental and calculated results show that the channel height as well as the hard plate do not give any significant effects on the flutter start velocity. Comparing Figs.12 and 13 with Fig.9, however, the calculated flutter reduced frequency is three to four times as much as the experimental one for the rubber plate. Huang also showed that the flutter frequency of a natural rubber plate was nearly one-third of that of a plastic thin plate (given in Fig.12). Hence, this remarkable discrepancy between the calculated and experimental ones may be attributed to the effect of material mechanical damping, which is large in rubber plate but not in plastic plate(cf.Fig.8).

From the consideration on a simple mass-spring system, the energy dissipation for one cycle of the oscillation of unit amplitude is approximately estimated as

$$W \sim \left( \frac{m}{\pi \rho \ell^2} \right) \left( \frac{\omega \ell}{U} \right)^2 \delta \quad (7)$$

where  $m$  and  $\ell$  are the mass and characteristic length of the oscillating body.

Applying this damping effect to the present calculation, the flutter will occur when  $E+W < 0$  holds. For the case of the natural-rubber plate (e.g. 100 mm long and 1mm thick), the mass ratio  $(m/\pi \rho \ell^2)$  is of the order around 5 and the logarithmic damping coefficient  $\delta$  is about 0.5 (see Table 1). Assume  $W = 5(\omega \ell_s/U)^2$ , and the flutter reduced frequency  $(\omega \ell_s/U)_r$  for  $\phi = 2.0$  is estimated as around 0.9. This suggests that mechanical damping gives a predominant effect on flutter of the soft plate, and also that the theoretical approach could be applied to the prediction of flutter of soft plate, if the mechanical damping is estimated properly.